

Synthesis, Properties and *In Vitro* Photodynamic Activity of Water-soluble Azaphthalocyanines and Azanaphthalocyanines

Petr Zimcik¹, Miroslav Miletin¹, Hana Radilova², Veronika Novakova¹, Kamil Kopecky¹, Jaroslav Svec¹ and Emil Rudolf³

¹Department of Pharmaceutical Chemistry and Drug Control, Faculty of Pharmacy in Hradec Kralove, Charles University in Prague, Hradec Kralove, Czech Republic

²GENERI BIOTECH s.r.o., Hradec Kralove, Czech Republic

³Department of Medical Biology and Genetics, Faculty of Medicine in Hradec Kralove, Charles University in Prague, Hradec Kralove, Czech Republic

Received 29 May 2009, accepted 11 September 2009, DOI: 10.1111/j.1751-1097.2009.00647.x

ABSTRACT

In this work zinc azaphthalocyanines (AzaPcs) from the group of tetrapyrazinoporphyrazines and zinc azanaphthalocyanines from the group of tetra[6,7]quinoxalinoporphyrazines (TQP) with eight diethylaminoethylsulfanyl substituents were synthesized. Tertiary amines were later quaternized with ethyl iodide to obtain water-soluble photosensitizers (PSs). Quaternized compounds showed high singlet oxygen quantum yields as determined in DMF by monitoring decomposition of 1,3-diphenylisobenzofuran. In water medium, quaternized AzaPc derivatives appeared in monomeric form in a wide range of concentrations while quaternized TQP derivatives showed aggregation at higher concentrations (over 1 μM). Photodynamic activity was tested on Hep2 cells using light of $\lambda > 640$ nm. Both quaternized dyes showed high photodynamic activity ($\text{IC}_{50} = 104$ and 220 nm for AzaPc and TQP, respectively). Dark toxicity was not detected even at the highest concentration used in *in vitro* tests (200 μM) which indicates a promising therapeutic index of these new substances. Tested compounds localized inside the cells mainly within the lysosomes thus suggesting an endocytic mechanism of cellular uptake. No localization within mitochondria was detected. A great advantage of TQP derivatives over other PSs is their very strong absorption at 747 nm that allows activation at wavelengths penetrating deeper into human tissues.

INTRODUCTION

Photodynamic therapy (PDT) is a well-established method for the treatment of malignant and nonmalignant diseases which combines three basic components, *i.e.* photosensitizer (PS), light and oxygen with each of them being harmless when applied individually. The mechanism of action of PDT is based on the absorption of the light by PS and transfer of the energy to surrounding molecules, mainly oxygen (1–5). Cytotoxic species produced after illumination, most important of them being singlet oxygen ($^1\text{O}_2$), inflict damage to cells ultimately leading to their death.

The clinical history of PDT started in 1991 by approval of porfimer sodium (Photofrin[®]) in Canada for treatment of bladder cancer. However, its photophysical and pharmacokinetic properties are not optimal. This complicated mixture of oligomers absorbs light at only 630 nm with low extinction coefficient ($\epsilon \sim 2000 \text{ M}^{-1}\text{cm}^{-1}$) and causes prolonged (up to 6 weeks) skin photosensitivity. These aforementioned drawbacks have prompted the development of new PSs and some of these second-generation PSs have been already accepted in clinical practice (verteporfin, temoporfin, talaporfin, aminolevulinic acid, methyl- and hexyl-aminolevulinic acid) (2,6,7). The second-generation compounds are defined chemical individuals with stronger absorption at longer wavelengths, short-lasting skin photosensitivity and low dark toxicity. Of particular importance appears to be their longer wavelength of absorption as lower wavelengths are strongly absorbed by endogenous chromophores (*e.g.* hem) and, consequently, the penetration of red light (~ 630 nm) is rarely greater than 5 mm while it can be as high as 1–2 cm with longer wavelengths (≤ 800 nm) (7).

Phthalocyanines (Pcs) are among the most promising groups of new PSs receiving increased attention in the last few years. They absorb strongly ($\epsilon \sim 150\,000$ – $200\,000 \text{ M}^{-1}\text{cm}^{-1}$) at longer wavelengths (close to 700 nm) and are characterized by good singlet oxygen quantum yields (Φ_{Δ}) which is why they were subject to a number of biological tests. Photodynamic activity of several new zinc and silicon Pcs was investigated *in vitro* on different cell lines (8–11) as well as against pathogenic microorganisms (12,13) and results showed promise. In addition, biological tests of sulfonated ZnPc *in vivo* on Wistar rats were performed recently (14). Pilot studies with a long time known silicon Pc4 have recently been conducted on animals (15) as well as deep investigations into its activity and mechanism of action have been carried out (16–19). Lastly, a mixture of sulfonated aluminum Pcs (Photosens) has already been approved in Russia for cancer treatment since 2001. Although the photophysical and photochemical properties of Pcs are very promising, their common problems are low solubility in water and strong tendency of this planar macrocyclic system to aggregation. These problems are usually solved by using different additives such as organic solvents (20) or Cremophor EL (10) that are not, however, devoid of their own toxicity.

*Corresponding author email: petr.zimcik@faf.cuni.cz (Petr Zimcik)

© 2009 The Authors. Journal Compilation. The American Society of Photobiology 0031-8655/10

Our own research has been focused on the aza analogs of Pcs—azaphthalocyanines (AzaPcs) from the group of tetrapyrroloporphyrins. We have uncovered several relationships between the structure of AzaPcs and their photophysical properties (21,22). AzaPc macrocycle can be also enlarged for next benzene rings yielding azanaphthalocyanines (AzaNcs) from the group of tetraquinoxalinoporphyrazines (TQP). These compounds absorb light at wavelength around 750 nm and thus can be very suitable as modern PSs with a deeper therapeutic hit. Although the photophysical and other properties of AzaPcs in organic solvents have been largely investigated by several groups (23–26), no photodynamic activity on cells has been studied yet. Furthermore, TQPs are still very rarely mentioned in the literature and only few researchers have described the synthesis and some basic photophysical properties of these interesting compounds (27–29). We present here synthesis, characterization, aggregation behavior, photophysical and photochemical properties and *in vitro* photodynamic tests on Hep2 cells of water-soluble AzaPcs and TQPs.

MATERIALS AND METHODS

General. All organic solvents used for the synthesis were of analytical grade. Anhydrous dimethylformamide (DMF) was purchased from Acros, diethylaminoethanethiol hydrochloride and 1,3-diphenylisobenzofuran (DPBF) from Aldrich. Zinc(II) phthalocyanine (ZnPc) was obtained from Eastman Organic Chemicals (New York). All chemicals were used as received except for zinc(II) acetate dihydrate (Lachema, Czech Republic) which was dried at 78°C under reduced pressure (13 mbar) for 5 h. TLC was performed on Merck aluminum sheets with silica gel 60 F254. Merck Kieselgel 60 (0.040–0.063 mm) was used for column chromatography. Melting points were measured on Electrothermal IA9200 Series Digital Melting point Apparatus (Electrothermal Engineering Ltd., Southend-on-Sea, Essex, UK) and are uncorrected. Infrared spectra were measured in KBr pellets on IR-Spectrometer Nicolet Impact 400. ¹H and ¹³C NMR spectra were recorded on Varian Mercury-Vx BB 300 (299.95 MHz—¹H; 75.43 MHz—¹³C). Chemical shifts reported are given relative to internal Si(CH₃)₄. Elemental analysis was performed on Elemental Analyser EA1110 (Carlo Erba Instruments). UV–Vis spectra were recorded on spectrophotometer UV-2401PC (Shimadzu Europa GmbH, Duisburg, Germany). MALDI-TOF mass spectra were recorded in positive reflectron mode on a mass spectrometer Voyager-DE STR (Applied Biosystems, Framingham, MA). For each sample, 0.5 μL of the mixture was spotted onto the target plate, air-dried and covered with 0.5 μL of matrix solution consisting of 10 mg of α-cyano-4-hydroxycinnamic acid in 100 μL of 50% ACN in 0.1% trifluoroacetic acid. The instrument was calibrated externally with a five-point calibration using Peptide Calibration Mix1 (LaserBio Labs, Sophia-Antipolis, France). Compounds **1** (30), **10** (31) and **11** (31) were synthesized according to published procedures. For modified procedure of synthesis of **9**, see Supporting Information.

Synthesis. 2,3,9,10,16,17,23,24-Octakis(2-(triethylammonio)ethylsulfanyl) tetrapyrroloporphyrin zinc(II) octaiodide (**2**)—compound **1** (82 mg, 50 μmol) was dissolved in ethyl iodide (10 mL) and the solution was stirred at room temperature (rt) for 2 days. The green precipitate, which appeared after 2 days, was dissolved after addition of *N*-methylpyrrolidinon (14 mL) and the reaction was stirred for the next 5 days at rt. The green solution was poured into diethylether, resulting precipitate collected and washed thoroughly with diethylether and acetone. Thereafter the product was dissolved in MeOH, filtered and the solvent was evaporated. The product was recrystallized from MeOH/diethylether. Yield was 137 mg (95%) of green solid. ¹H NMR (D₂O + C₅D₅N) δ = 4.74–4.50 (broad, 16H, S-CH₂), 4.20–3.96 (broad, 16H, N-CH₂), 3.94–3.66 (broad, 48H, N-CH₂), 1.82–1.54 (broad, 72H, CH₃); ¹³C NMR (D₂O + C₅D₅N) δ = 55.6, 53.2, 30.0, 7.4 (aromatic signals not detected); IR (KBr) ν = 2976, 1728, 1658, 1517, 1452, 1395, 1304, 1250, 1175, 1108, 1094, 971; UV–Vis (H₂O)

λ_{max} (ε) 652 (169 000), 592 (25 000), 376 (112 000); Anal. Calc. for C₈₈H₁₅₂I₈N₂₄S₈Zn + 3H₂O: C 35.98, H 5.42, N 11.44 Found: C 36.17, H 5.52, N 11.20.

2,3,11,12,20,21,29,30-Octakis(2-(diethylamino)ethylsulfanyl)tetra-[6,7]-quinoxalinoporphyrazine zinc(II) (**3**)—magnesium turnings (196 mg, 8.16 mmol) were refluxed in dry butanol (15 mL) with a small crystal of iodine for 3 h. Compound **12** (508 mg, 1.15 mmol) was added and reflux continued for next 24 h. Butanol was evaporated and the product extracted from the resulting solid using THF. After evaporation of THF, the solid was washed thoroughly with hot MeOH yielding a blue solid (200 mg, 39%). This magnesium TQP was dissolved in 2% aqueous HCl (50 mL) with the use of ultrasound and stirred at rt for 45 min. The solution was neutralized with concentrated Na₂CO₃ solution and made basic with few drops of NaOH. The green precipitate was collected and washed with water and hot MeOH yielding metal-free TQP (184 mg, 93%). The metal-free TQP was dissolved in pyridine (30 mL), anhydrous zinc acetate (1.83 g, 10 mmol) was added and the mixture was refluxed for 45 min. Pyridine was evaporated and the mixture was washed with water. The green solid was then dissolved in 2% aqueous HCl, filtered and made basic with NaOH. The green precipitate was collected and washed thoroughly with water and hot MeOH. Yield 180 mg (95%). ¹H NMR (C₅D₅N) δ = 9.81 (s, 8H, ArH), 4.54–3.83 (broad, 16H, S-CH₂), 3.44–3.26 (broad, 16H, N-CH₂), 2.95 (q, 32H, J = 7 Hz, N-CH₂), 1.37 (t, 48H, J = 7 Hz, CH₃); ¹³C NMR (C₅D₅N) δ = 156.6, 152.5, 140.3, 136.9, 121.3, 52.1, 47.4, 30.0, 12.6; IR (KBr) ν = 2996, 2800, 1633, 1568, 1515, 1452, 1384, 1340, 1309, 1255, 1131, 1022; MALDI-TOF *m/z* = 1832 [M]⁺, UV–Vis (pyridine) λ_{max} (ε) 752 (164 000), 693 (87 000), 382 (150 000); Anal. Calc. for C₈₈H₁₂₀N₂₄S₈Zn + 3H₂O: C 55.92, H 6.72, N 17.79 Found: C 55.82, H 6.49, N 17.83.

2,3,11,12,20,21,29,30-Octakis(2-(triethylammonio)ethylsulfanyl) tetra-[6,7]-quinoxalinoporphyrazine zinc(II) octaiodide (**4**)—compound **3** (87 mg, 47 μmol) was dissolved in ethyl iodide (11 mL) and the solution was stirred at rt for 2 days. The green precipitate, which appeared after 2 days, was dissolved after addition of *N*-methylpyrrolidinon (15 mL) and the reaction was stirred for next 5 days at rt. The green solution was poured into diethylether and precipitate collected, washed thoroughly with diethylether and acetone. The product was then dissolved in MeOH, filtered and evaporated. The product was recrystallized from MeOH/diethylether. Yield was 120 mg (90%) of a dark green solid. ¹H NMR (D₂O + C₅D₅N) δ = 10.0 (s, 8H, ArH), 5.08–4.85 (broad, 16H, S-CH₂), 4.16–3.57 (m, 64H, N-CH₂), 1.77–1.46 (m, 72H, CH₃); ¹³C NMR (D₂O + C₅D₅N) δ = 153.8, 151.8, 140.0, 121.4, 55.5, 53.4, 30.2, 7.5 (one aromatic signal overlapped with signal of the solvent); IR (KBr) ν = 2974, 1630, 1452, 1384, 1339, 1255, 1131, 1022; UV–Vis (DMF) λ_{max} (ε) 748 (372 000), 712 (43 000), 669 (43 000), 389 (154 000); Anal. Calc. for C₁₀₄H₁₆₀I₈N₂₄S₈Zn + 4H₂O: C 39.58, H 5.37, N 10.65 Found: C 39.19, H 5.28, N 10.50.

2,3-bis(2-(diethylamino)ethylsulfanyl)quinoxaline-6,7-dicarbonitrile (**12**)—diethylaminoethanethiol hydrochloride (849 mg, 5 mmol) was dissolved in water (10 mL), 1 M aqueous solution of NaOH (10 mL, 10 mmol) was added and the solution stirred at rt for 15 min. 2,3-dichloroquinoxaline-6,7-dicarbonitrile (**11**) was added (500 mg, 2 mmol) dissolved in THF (100 mL). The solution turned yellow and was stirred at rt. THF was evaporated after 1 h of stirring, few drops of NaOH were added (to basic reaction) to the remaining water suspension and the solid was filtered and washed with water. The yellow-brown solid was dissolved in diethylether and washed with water which was made basic with few drops of NaOH. Afterward, diethylether solution was washed with acidic solution (water + HCl) and discarded. The acidic water solution was made basic with NaOH, washed with diethylether several times and the organic layer was dried (Na₂SO₄). Diethylether was evaporated and a yellow solid recrystallized from MeOH yielding 560 mg (62%) of yellow needles. M.p. 127.8–128.7°C (MeOH); ¹H NMR (CDCl₃) δ = 8.23 (s, 2H, ArH), 3.45 (t, 4H, J = 7 Hz, S-CH₂), 2.83 (t, 4H, J = 7 Hz, N-CH₂), 2.65 (q, 8H, J = 7 Hz, N-CH₂), 1.09 (t, 12H, J = 7 Hz, CH₃); ¹³C NMR (CDCl₃) δ = 161.0, 140.2, 134.3, 115.3, 112.2, 50.9, 47.1, 28.9, 12.0; IR (KBr) ν = 3097, 3073, 3027, 2970, 2934, 2874, 2798, 2237 (CN), 1507, 1470, 1386, 1290, 1265, 1195, 1124, 1069, 1030. Compound **12** was converted to its hydrochloride after dissolution in acetone/diethylether 1:3 and bubbling with

gaseous HCl. A white-yellow precipitate was collected and recrystallized from MeOH/diethylether. M.p. slowly decomposed from 200°C.

Hydrochlorides of 1 and 3—general procedure. Dye **1** or **3** (1 μmol) was dissolved or suspended in THF (5 mL) and MeOH (1 mL) and concentrated HCl (0.5 mL) was added. Any remaining solid dissolved after the addition of HCl. The mixture was stirred at rt for 30 min, toluene (5 mL) was added and solvents were evaporated to dryness. The sample was dried under deep vacuum (4 mbar) at 50°C for 45 min and used directly for preparation of solutions used for biological tests.

Fluorescence and singlet oxygen. Singlet oxygen quantum yields were determined according to a previously published procedure using decomposition of a chemical trap of singlet oxygen DPBF (32). Absorption of the dyes in Q-band area during measurements was approximately 0.1. ZnPc was used as the reference ($\Phi_{\Delta} = 0.56$ in DMF [30,33]). In some cases HCl was added to a final concentration of 5×10^{-4} M. This addition did not influence the quantum yields of standard ZnPc in DMF as was shown before (30). For more details see Supporting Information. Fluorescence quantum yields were determined by comparative method using ZnPc as the reference ($\Phi_{\text{F}} = 0.20$ in pyridine [34]). To minimize reabsorption effect, absorption of the dyes in the Q-band area was kept below 0.05, excitation wavelength was 375 nm.

Cell lines. For photodynamic activity, Hep2 (Human Negroid cervix carcinoma) cells were obtained from the European Collection of Cell Cultures (No. 86030501, Salisbury, UK). Cells were maintained in Dulbecco's modified Eagle's medium (Cambrex, Walkersville, MD) with L-glutamine and glucose, supplemented with 10% fetal bovine serum (PAA Laboratories GmbH, Pasching, Austria) and gentamicin ($50 \mu\text{g mL}^{-1}$; Sigma-Aldrich, St. Louis, MO), and were grown at 37°C in an atmosphere containing 5% CO_2 . The cell line was tested for mycoplasma contamination.

Phototoxicity assay. Photosensitizers **1–4** were dissolved in PBS to a stock concentration 100 μM for phototoxicity or 1 mM for dark toxicity tests and diluted further with PBS. The stock solutions were filtered through 0.2 μm filters. Cells were seeded at 1×10^4 cells/well in a 96-well plate. The day after, the PSs were added and incubated with cells for 15 min, 90 min or 4 h. After incubation, cells were rinsed with PBS, covered with fresh medium and irradiated (58 mW cm^{-2} , 15 min). To avoid any important dilution of medium with PBS, the amount of added PBS with dyes remained at 1% (phototoxicity) or 20% (dark toxicity) with respect to the volume of medium in the well. Maximal concentrations of the dyes in tests were therefore 1 and 200 μM for phototoxicity and dark toxicity, respectively. Irradiation was performed using a 250 W QTH (Quartz Tungsten Halogen) lamp (Oriol Instruments). Light was filtered through a heat filter and cut on 640 nm filter. Twenty-four hours after irradiation, the cell viability was determined using Cell Counting Kit-8 (ALEXIS Corporation, Lausen, Switzerland). The experiments were performed in triplicate for each concentration. Cells grown in the culture medium diluted with an appropriate amount of PBS without any dye were taken as control (100% viability). Dark toxicity was tested with 24 h incubation of dyes with cells and without any irradiation and protected from light.

Fluorescence microscopy and image analysis. The 100 μM stock solutions of compounds **1–4** in PBS were diluted in cultivation medium to the final concentration of 10 μM and Hep2 cells grown in cytospin chambers were exposed to them for 12 h. Prior to visualization of fluorescence, cells were exposed to MitotrackerGreen (Invitrogen-Molecular Probes, Inc., Carlsbad, CA; 50 nm, 25 min, 37°C) or LysotrackerBlue (Invitrogen-Molecular Probes, Inc.; 25 nm, 25 min, 37°C), rinsed with PBS and mounted. The localization and intensity of fluorescence were examined under wide-field fluorescence microscope (Nikon Eclipse E 400; Nikon Corporation, Kanagawa, Japan) equipped with the digital color matrix camera COOL 1300 (VDS; Vosskühler, Osnabrück, Germany), using Texas Red (EX 540-580 and BA 600-660), Cy5-HYQ (EX 590-650 and BA 663-738) and UV (EX 330-380 and BA 420) specific filters. Photographs were taken independently using LUCIA DI Image Analysis System LIM (Laboratory Imaging Ltd., Prague, Czech Republic). Image and colocalization analyses were carried out with help of Lucia NIS-Elements AR 2.30 or Image J. Fluorescence was finally combined with phase contrast. For the purpose of analysis, at least 2000 cells were scored at 400 \times magnification.

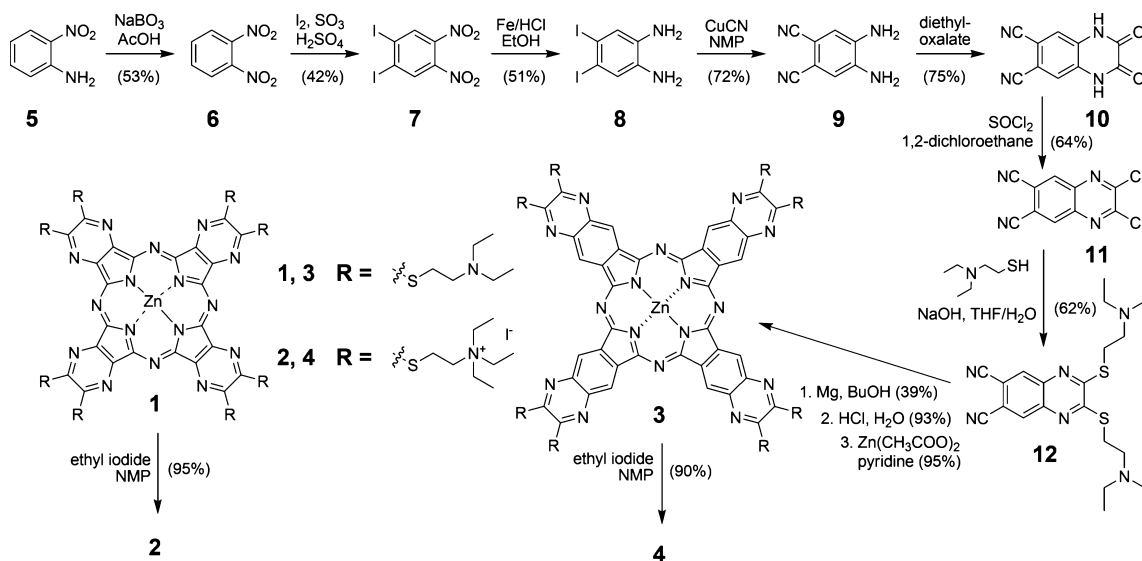
RESULTS AND DISCUSSION

Design of the molecules

We designed our molecules according to the previously discovered relationships which are further discussed in this paragraph. As mentioned above, aggregation of AzaPc and AzaNc is well known and may constitute a problem for photodynamic action. Aggregated PSs fail in efficient photosensitization as the excited states are relaxed rather through internal conversion than through intersystem crossing. Singlet oxygen quantum yields (Φ_{Δ}) are therefore strongly lowered and the compound loses its photodynamic potential. Aggregation in organic solvents is usually suppressed by introducing bulky substituents preventing self-association (22). A slightly different approach is considered in water medium where charged substituents are used for prevention of the stacking. Thus our intention was to prepare AzaPc and TQP with quaternary ammonium groups inhibiting the aggregation. In the previous photophysical study we showed that eight charged substituents are necessary for complete monomerization of AzaPc in water (30). The heteroatom connecting the macrocycle system considerably influences Φ_{Δ} and we showed that alkylsulfanyl derivatives are among the best singlet oxygen producers (21). Considering the central metal, zinc appears to be the most suitable because it increases the triplet state lifetimes resulting in very high Φ_{Δ} . Other central metals (Si, Al, Ge, Sn [35]) or metal-free derivatives (36) were investigated for photodynamic effect too and such Pcs showed good outcome in spite of their much lower Φ_{Δ} values. However, zinc is the metal of choice in order to maximize the photophysical and photochemical properties. AzaNcs of the TQP group form two isomers considering the position of nitrogen atoms in the structure—tetra[2,3]quinoxalino-porphyrazines and tetra[6,7]quinoxalino-porphyrazines. The latter isomers showed a much stronger bathochromic shift in the main absorption band (27,31) and therefore they were chosen for this application. We then decided to synthesize and test molecules **2** and **4** (Scheme 1).

Synthesis

Synthesis of TQP derivatives requires suitably substituted quinoxaline-6,7-dicarbonitriles. Recently, we described the synthesis of an important precursor **11** from 4,5-diaminophthalonitrile **9** (31). 4,5-diaminophthalonitrile **9** was prepared by the modified Youngblood's procedure (Scheme 1) (37). Chlorines in compound **11** are easily exchangeable by nucleophiles under mild conditions and thus its reaction with 2-(diethylamino)ethanethiolate at rt gave rise to **12** in a good yield. Compound **12** was stored in the form of hydrochloride due to stability reasons described previously for similar pyrazine homolog (30). Cyclotramerization of **12** using magnesium butoxide led to Mg complex of corresponding TQP which was then converted to the metal-free derivative. Insertion of zinc into the center of the macrocycle yielded compound **3**. Alkylation of **3** in ethyl iodide led to desired compound **4**. During alkylation, partially alkylated **3** precipitated from ethyl iodide that was used as alkylating agent and solvent at the same time. To ensure further alkylation in solution, *N*-methylpyrrolidinon was added to the reaction after 2 days



to support solubilization of the partially alkylated TQP. It is noteworthy that the complete synthetic procedure from **5** to compound **4** (Scheme 1) is very efficient, work up is simple and none of the reaction steps require chromatographic purification. AzaPc **1** has been prepared and described by us previously (30) and its alkylation to **2** followed the same procedure as for its TQP homolog. All analytical methods confirmed the structure and purity of the compounds. Compounds **1** and **3** were also converted to the corresponding hydrochlorides to allow their water solubility for biological tests.

UV-Vis absorption and aggregation

Compounds **1** and **3** are soluble in most organic solvents while alkylated homologs **2** and **4** are well soluble in water and polar organic solvents (methanol, DMF, $c_{\max} > 5$ mM for both solvents). Electronic absorption spectra of AzaPcs (**1** and **2**) showed typical B-band around 375 nm and sharp Q-band with vibrational bands at 655 nm. TQP homologs (**3** and **4**) absorb at wavelengths longer by 90 nm (Table 1). This important redshift caused by enlargement of the macrocyclic system allows them to absorb the light at wavelengths with potential of deeper penetration through human tissues.

AzaPcs **1** and **2** do not aggregate in DMF or pyridine and **2** is nonaggregated in water too, a feature which is only rarely seen for ZnPcs and ZnAzaPcs. The shape of the absorption spectrum

in water corresponded well to the spectrum in DMF (Fig. 2a), it did not change its shape at higher concentrations and obeyed Lambert-Beer law in a wide range of concentrations (Fig. 1a).

Table 1. Photophysical and photochemical data of investigated compounds in DMF.

Compound	λ_{\max} (nm)	λ_{em} (nm)	Φ_{F}^*	Φ_{Δ}^{\dagger} (DMF)	Φ_{Δ}^{\dagger} (DMF/HCl)
1	655	661	0.004 \ddagger	0.039 \ddagger	0.467 \ddagger
2	656	661	0.058	0.196	0.726
3	745	750	0.007 \S	0.410 \S	0.478 \S
4	748	751	0.027	0.754	0.677

*ZnPc reference (Φ_{F} in pyridine 0.20 [34]). \dagger ZnPc as reference (Φ_{Δ} in DMF 0.56 [30,33]). \ddagger Data from Ref. (30). \S Aggregation.

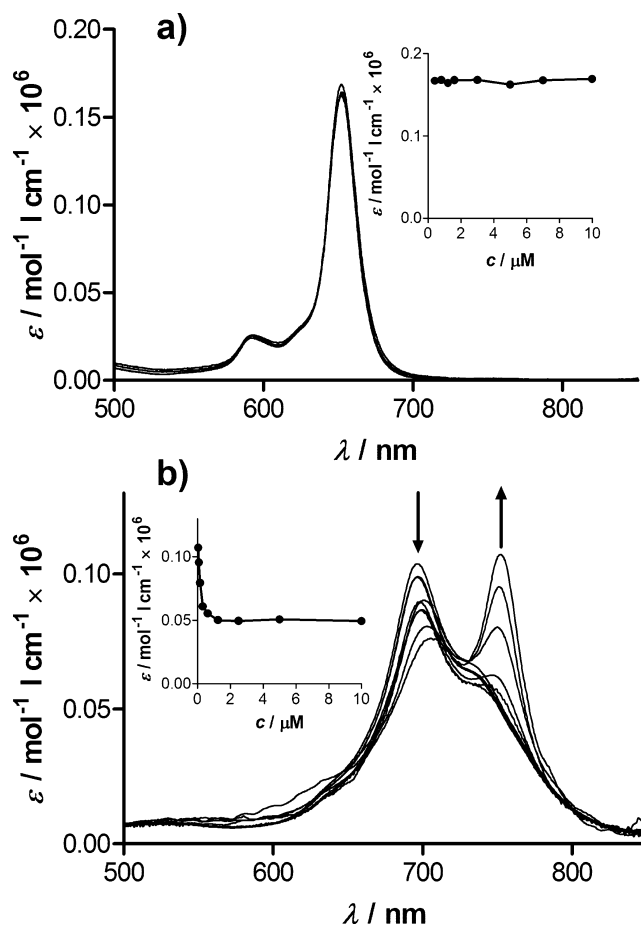


Figure 1. Absorption spectra of compounds **2** (a) and **4** (b) in water at different concentrations ranging from 10 μM to 0.04 μM . Insets: dependence of ϵ at Q-band maximum of monomer (652 nm for **2**, 755 nm for **4**) on the concentration.

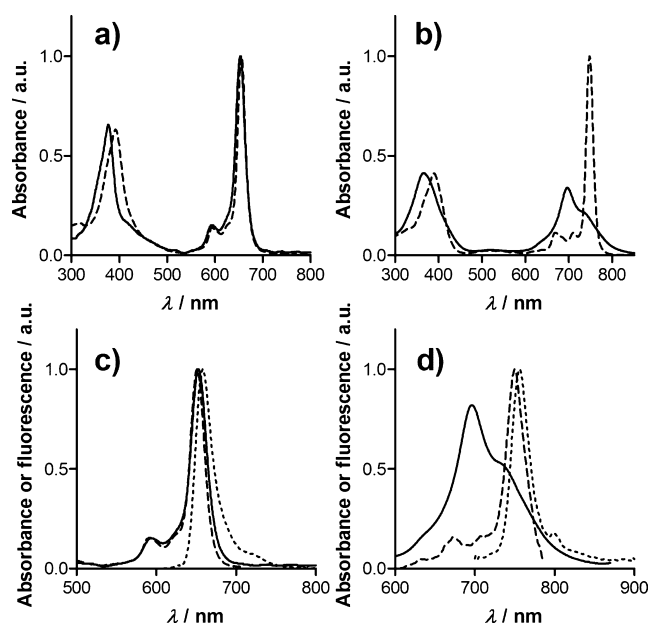


Figure 2. (a) Absorption spectra of **2** in DMF (dashed) and water (full), (b) absorption spectra of **4** in DMF (dashed) and water (full), (c) absorption (full), excitation (dashed) and emission (dotted) spectra of **2** in water, (d) absorption (full), excitation (dashed) and emission (dotted) spectra of **4** in water.

On the other hand, the enlarged macrocyclic system of TQP **3** tends to aggregate even in DMF or pyridine. Its spectrum in pyridine changes with dilution and with higher temperature that is typical of the presence of aggregates (see Supporting Information). Quaternization of **3** reduced aggregation in organic solvents and compound **4** was found to be fully monomeric in DMF or MeOH. However, its water solution showed the presence of aggregates at higher concentrations as it changed its spectrum in Q-band area with dilution and did not follow Lambert–Beer law (no constant extinction coefficient, Fig. 1b). Significant monomerization started below $1 \mu\text{M}$ (Fig. 1b, inset). Higher temperature or addition of organic solvent (pyridine, DMF or MeOH) into water helped in monomerization too (see Supporting Information).

Fluorescence and singlet oxygen

Fluorescence emission spectra of all the studied compounds were of the typical shape for AzaPc and similar compounds with only a small Stokes shift (Table 1). In the case when compounds were present as monomers, their excitation spectra corresponded well to absorption spectra (DMF solutions of **1**, **2** and **4** and water solution of **2** [see Fig. 2a,c]). In the case when aggregates were detected in UV–Vis spectra (**3** in DMF or pyridine, **4** in water [see Fig. 2b,d]) the excitation spectra differed from UV–Vis absorption spectra. The aggregates formed in solution alter significantly the absorption spectrum. The fluorescence excitation spectrum is not influenced because the aggregates usually do not fluoresce besides few exceptions of J-dimers (38,39). Titration of aggregated water solution of **4** with pyridine resulted in a change in the electronic absorption spectra shape but it had no effect on fluorescence emission and excitation spectra. Only an increase in fluorescence intensity was observed.

Fluorescence quantum yields (Φ_F) (Table 1) were relatively low for all compounds, in particular for nonalkylated compounds **1** and **3**, that can be explained by efficient photoinduced electron transfer (PET) and aggregation (see below).

Singlet oxygen quantum yields (Φ_Δ) were determined by observing the decomposition of its chemical trap DPBF. Results are summarized in Table 1. Proper interpretation of the results is complicated because they are influenced by two factors—PET and aggregation. As shown by other authors, PET from amines to excited Pc macrocycle is responsible for quenching of Pc excited states (40) and as a result quantum yields of both singlet oxygen and fluorescence are lowered (9). Compound **1** has therefore low Φ_Δ in DMF which is, however, increased after the addition of HCl into solution. Hydrochloric acid protonates amines which are not further available as donors for PET. Alkylated AzaPc **2** has higher Φ_Δ in DMF than **1** as a consequence of PET inhibition by quaternization but after addition of HCl its Φ_Δ reaches an even higher value of 0.726 typical of alkylsulfanyl AzaPcs (30). It seems therefore that some of the amines may not be alkylated, although we have no analytical support for this fact. As the effect of PET is very strong, it may involve just one or even less nonalkylated amino group per one molecule of AzaPc. Still, it shall not constitute a problem for proper biological evaluation of this compound as one possible free amino group will be fully protonated in water medium at pH 7.4 and therefore no PET will occur. It should be noted that both **1** and **2** were fully monomeric during all measurements and that is why aggregation did not account for changes in Φ_Δ and Φ_F values.

TQP enlarged system does not allow efficient PET due to longer distance between donor and acceptor and therefore Φ_Δ value of **3** in DMF is 0.410. However, its Φ_Δ values are lowered by observed aggregation of this compound in both DMF and DMF with HCl. Inefficient PET and monomeric state of **4** lead to very high Φ_Δ values of about 0.7 in both DMF and DMF/HCl. The values for **4** are similar in both solvent systems and a possible small difference may be attributed to experimental error. The above-mentioned facts emphasize the important role of quaternization (aside from an increase in water solubility) in preserving the good photochemical properties of AzaPc PSs substituted with amines.

Photodynamic activity

Photodynamic activity and toxicity were tested on Human Negroid cervix carcinoma cells Hep2. Compounds **2** and **4** as well as hydrochlorides of **1** and **3** were tested after dissolution in PBS. No organic solvent or any other additives like surfactants were added. As shown in Table 2 no dark toxicity

Table 2. Biological activities of AzaPc and TQP on Hep2 cells.

Compound	Dark toxicity [†] (IC ₅₀ in μM)	Phototoxicity [‡] (IC ₅₀ in μM)
1 *	37	> 1.0
2	> 200	0.104
3 *	> 200	0.273
4	> 200	0.220

AzaPc = azaphthalocyanine; TQP = tetra[6,7]quinoxalinoporphyrazine. *Applied in the form of hydrochlorides. [†]Incubation for 24 h. [‡]Irradiation after 4 h of incubation.

was detected after 24 h treatment up to 200 μM which was a maximal concentration used in tests. It shows the very low toxicity of prepared dyes in the absence of light. The only exception was hydrochloride of **1** which showed IC_{50} at 37 μM . The IC_{50} values are defined as the dye concentration required to kill 50% of the cells.

The photodynamic activity of tested compounds was determined after 4 h of incubation. The uptake time was based on the experiment where compound **3** and quaternary **4** were incubated with cells for different times and irradiated ($\lambda > 640 \text{ nm}$, 58 mW cm^{-2} , 15 min). The determined IC_{50} values were 279, 117 and 220 nM for **4** and >1000 , 238 and 273 nM for **3** for 15 min, 90 min and 4 h, respectively. Although very high photodynamic activity was observed after 90 min treatment, thus indicating rapid uptake, the 4 h incubation was chosen to allow full incorporation. Results of photodynamic activity tests are summarized in Table 2 and Fig. 3.

In accordance with the above discussed results of photochemical measurements and aggregation properties, the strongest effect was observed for quaternized compound **2** followed by **4**, *i.e.* compounds which were originally designed as the optimal compounds. Lower activity of **4** can be attributed to its higher tendency to aggregate in water medium when compared with **2**. Amino groups of **1** and **3** in water medium (pH 7.4) should be found in equilibrium between ionized and nonionized forms. According to the Henderson–Hasselbalch equation (41) and estimated pK_a value 9.38 ± 0.25 of amino groups (calculated using Advanced Chemistry Development [ACD/Labs] Software V9.04 for Solaris), at least one of eight amino groups will be nonionized. It may lead to quenching of excited states of **1** by PET and to very low photodynamic activity. As no PET occurs in **3**, its photodynamic activity is comparable to quaternized homolog **4**.

Subcellular localization

There have been several reports on the localization of cationic Pc in subcellular compartments, especially in lysosomes (8) or mitochondria (9,42). The subcellular localization was studied after 12 h incubation in dark and analyzed together with organelle-specific probes for lysosomes and mitochondria. As shown in Fig. 4 for compound **2**, the localization of the specific fluorescence signals suggests the diffuse accumulation of **2** in

the cytoplasm where it colocalizes mainly with lysosomes as indicated by image analysis. Conversely, no significant colocalization with mitochondria was found. In addition, the observed topography of intracellular distribution of **2** seems to

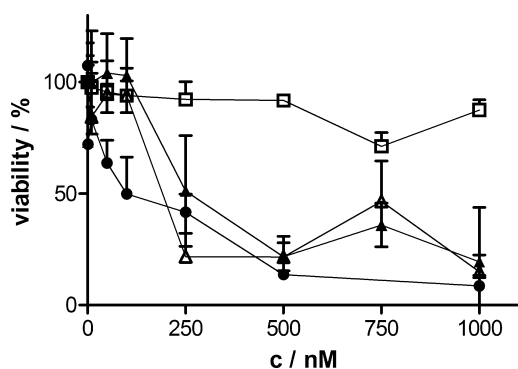


Figure 3. Viability of Hep2 treated with a range of concentrations of the photosensitizers **1** (□), **2** (●), **3** (Δ) and **4** (▲) after irradiation ($\lambda > 640 \text{ nm}$) for 15 min at a fluence rate of 58 mW cm^{-2} . Mean of triplicate experiments. Error bars represent standard deviation.

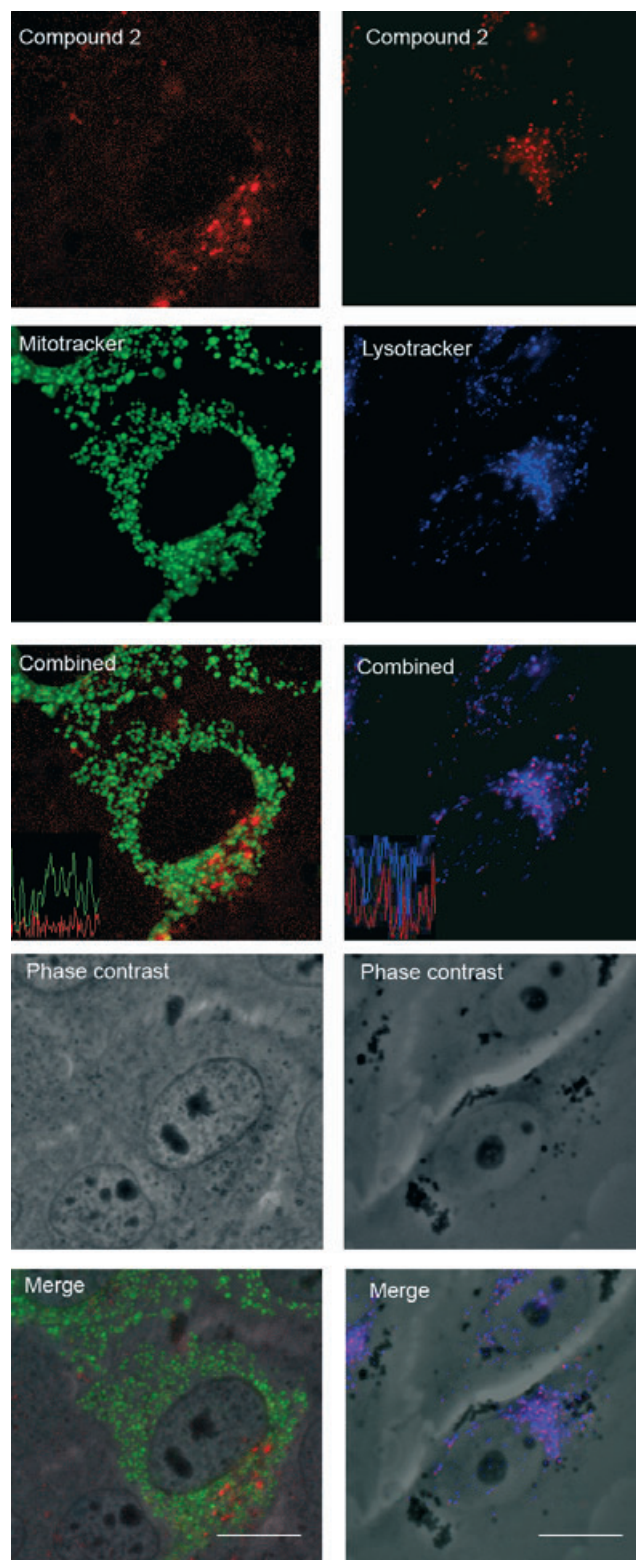


Figure 4. Fluorescence and phase contrast microscopy of compound **2** in Hep2 cells, 400 \times . Bar 5 μm .

rule out any significant accumulation or specific binding of this compound to the cell membrane. The localization of this highly charged compound in lysosomes can be anticipated and shows an endocytic mechanism of cellular uptake. The tests were performed also with other dyes (**1**, **3** and **4**) and the results indicated a similar behavior (see Supporting Information). Unfortunately, their low fluorescence signal, a consequence of very low Φ_F , did not allow unequivocal conclusions to be made.

CONCLUSION

In conclusion, we synthesized quaternized AzaPc and TQP that are well soluble in water and are found in this solution mainly in the monomeric state at high concentrations (**2**) or at low concentrations (**4**). Both dyes are characterized by high singlet oxygen quantum yields that make them promising PSs for PDT. Quaternization of peripheral amines appeared to be crucial for good photodynamic activity of AzaPc molecules as deduced from lower singlet oxygen quantum yields and hardly detected photodynamic activity of nonquaternized AzaPc **1**. The reason for the lower activity is most likely based on deactivation of AzaPc excited states by intramolecular PET. Photodynamic activity of similar TQP macrocycle **3** is almost not influenced as a consequence of ineffective PET. Also, we present here the results of the first *in vitro* photodynamic tests of these types of PSs. Their photodynamic activity on Hep2 cells was found to be strong and they did not require any special solubilizing agent to be added. Compounds **2** and **4** possess promising therapeutic index as they were found to be nontoxic in the dark up to the maximum used concentration 200 μM (*i.e.* more than 1000 times less effective than toxic concentration) and localize inside the cells mainly in lysosomes. Compound **4** has strong absorption at long wavelengths close to 750 nm that allows excitation with light having deeper penetration through human tissues and that is why larger tumors could be treated. Therefore we believe that this particular compound has high potential to become a very attractive alternative to established PS.

Acknowledgements—This work was supported by Research Project MSM0021620822, Czech Science Foundation Grant No. 203/07/P445 and Czech Academy of Sciences, Prague, Grant No. KAN200100801. Cytotoxic and photodynamic tests were performed by GENERI BIOTECH s.r.o. and their help is highly acknowledged.

SUPPORTING INFORMATION

Additional Supporting Information may be found in the online version of this article:

Figure S1. Changes in absorption spectra of **3** in pyridine at 1.0 μM with increasing temperature.

Figure S2. Changes in absorption spectra of **3** in pyridine with dilution from 10 μM to 0.3 μM at rt. Inset: Values of extinction coefficient at 752 nm in dependence on concentration.

Figure S3. Changes in absorption spectra of **4** in water at 2.2 μM with increasing temperature.

Figure S4. Changes in absorption spectra of **4** in water at 1.0 μM with increasing amount of pyridine (A), DMF (B) or MeOH (C) added into solution. Insets: Changes in absorbance at 756 nm.

Figure S5. Changes in fluorescence emission of **4** in water at 1.0 μM with increasing amount of pyridine added to solution (from 0% to 15% vol/vol). Excitation wavelength 375 nm. Absorption at excitation wavelength still remained the same (see Fig. S4A).

Figure S6. Changes in absorption spectra of DPBF after irradiation of its DMF solution containing compound **2** for 0, 15, 30, 80, 140 and 190 s. Inset: dependence of $\ln(A_0/A_t)$ on irradiation time t . A_0 is absorbance at 417 nm prior to irradiation, A_t is absorbance at 417 nm after irradiation for time t .

Figure S7. Fluorescence and phase contrast microscopy of compounds **1** and **2** in Hep2 cells, 400 \times . Bar 5 μm .

Figure S8. Fluorescence and phase contrast microscopy of compounds **3** and **4** in Hep2 cells, 400 \times . Bar 5 μm .

Modified synthesis of **9** (Figs. S1–S5) showing changes in absorption and fluorescence spectra of **3** and **4**, details on DPBF decomposition (Fig. S6) and figures of subcellular localization (Figs. S7 and S8) can be found.

Please note: Wiley-Blackwell are not responsible for the content or functionality of any supporting information supplied by the authors. Any queries (other than missing material) should be directed to the corresponding author for the article.

REFERENCES

- Triesscheijn, M., P. Baas, J. H. M. Schellens and F. A. Stewart (2006) Photodynamic therapy in oncology. *Oncologist* **11**, 1034–1044.
- Zimcik, P. and M. Miletin (2009) Photodynamic therapy. In *Dyes and Pigments—New Research* (Edited by A. R. Lang), pp. 1–62. Nova Science Publishers, New York.
- Castano, A. P., T. N. Demidova and M. R. Hamblin (2004) Mechanisms in photodynamic therapy: Part one—Photosensitizers, photochemistry and cellular localization. *Photodiagnosis Photodyn. Ther.* **1**, 279–293.
- Dougherty, T. J., C. J. Gomer, B. W. Henderson, G. Jori, D. Kessel, M. Korbelik, J. Moan and Q. Peng (1998) Photodynamic therapy. *J. Natl Cancer Inst.* **90**, 889–905.
- Qiang, Y. G., X. P. Zhang, J. Li and Z. Huang (2006) Photodynamic therapy for malignant and non-malignant diseases: Clinical investigation and application. *Chin. Med. J.* **119**, 845–857.
- Moreira, L. M., F. V. dos Santos, J. P. Lyon, M. Maftoum-Costa, C. Pacheco-Soares and N. S. da Silva (2008) Photodynamic therapy: Porphyrins and phthalocyanines as photosensitizers. *Aust. J. Chem.* **61**, 741–754.
- Wainwright, M. (2008) Photodynamic therapy: The development of new photosensitisers. *Anti-Cancer Agents Med. Chem.* **8**, 280–291.
- Li, H. R., T. J. Jensen, F. R. Fronczek and M. G. H. Vicente (2008) Syntheses and properties of a series of cationic water-soluble phthalocyanines. *J. Med. Chem.* **51**, 502–511.
- Lo, P. C., J. D. Huang, D. Y. Y. Cheng, E. Y. M. Chan, W. P. Fong, W. H. Ko and D. K. P. Ng (2004) New amphiphilic silicon(IV) phthalocyanines as efficient photosensitizers for photodynamic therapy: Synthesis, photophysical properties, and *in vitro* photodynamic activities. *Chem. Eur. J.* **10**, 4831–4838.
- Amerio, P., T. Gobello, C. Mazzanti, E. Giaculli, S. Ruggeri, D. Sordi, M. Amatetti, L. Chinni and A. Tulli (2007) Photodynamic therapy plus topical retinoids in Darier's disease. *Photodiagnosis Photodyn. Ther.* **4**, 36–38.
- Fabris, C., M. Soncin, G. Miotto, L. Fantetti, G. Chiti, D. Dei, G. Roncucci and G. Jori (2006) Zn(II)-phthalocyanines as phototherapeutic agents for cutaneous diseases. Photosensitization of fibroblasts and keratinocytes. *J. Photochem. Photobiol. B, Biol.* **83**, 48–54.

12. Scalise, I. and E. N. Durantini (2005) Synthesis, properties, and photodynamic inactivation of *Escherichia coli* using a cationic and a noncharged Zn(II) pyridyloxophthalocyanine derivatives. *Bioorg. Med. Chem.* **13**, 3037–3045.
13. Mantareva, V., V. Kussovski, I. Angelov, E. Borisova, L. Avramov, G. Schnurpfeil and D. Wöhrle (2007) Photodynamic activity of water-soluble phthalocyanine zinc(II) complexes against pathogenic microorganisms. *Bioorg. Med. Chem.* **15**, 4829–4835.
14. Zhang, Z. B., H. T. Jin, J. Bao, F. Fang, J. F. Wei and A. P. Wang (2006) Intravenous repeated-dose toxicity study of ZnPcS2P2-based-photodynamic therapy in Wistar rats. *Photochem. Photobiol. Sci.* **5**, 1006–1017.
15. Farooq, F. T., J. Berlin, E. Baron, A. L. Faulx, J. M. Marks and A. Chak (2007) Pilot animal study of the phthalocyanine Pc4 as a topically-applied photosensitizer for PDT of Barrett's esophagus. *Gastrointest. Endosc.* **65**, AB155.
16. Ahmad, N., K. Kalka and H. Mukhtar (2001) In vitro and in vivo inhibition of epidermal growth factor receptor-tyrosine kinase pathway by photodynamic therapy. *Oncogene* **20**, 2314–2317.
17. Ke, M. S., L. Y. Xue, D. K. Feyes, K. Azizuddin, E. D. Baron, T. S. McCormick, H. Mukhtar, A. Panneerselvam, M. D. Schluchter, K. D. Cooper, N. L. Oleinick and S. R. Stevens (2008) Apoptosis mechanisms related to the increased sensitivity of Jurkat T-cells vs A431 epidermoid cells to photodynamic therapy with the phthalocyanine pc 4. *Photochem. Photobiol.* **84**, 407–414.
18. Sakharov, D. V., E. D. R. Elstak, B. Chernyak and K. W. A. Wirtz (2005) Prolonged lipid oxidation after photodynamic treatment. Study with oxidation-sensitive probe C11-BODIPY581/591. *FEBS Lett.* **579**, 1255–1260.
19. Bai, L., J. Guo, F. A. Bontempo and J. L. Eiseman (2009) The relationship of phthalocyanine 4 (Pc 4) concentrations measured noninvasively to outcome of Pc 4 photodynamic therapy in mice. *Photochem. Photobiol.* **85**, 1011–1019.
20. Hofman, J. W., F. van Zeeland, S. Turker, H. Talsma, S. A. Lambrechts, D. V. Sakharov, W. E. Hennink and C. F. van Nostrum (2007) Peripheral and axial substitution of phthalocyanines with solketal groups: Synthesis and in vitro evaluation for photodynamic therapy. *J. Med. Chem.* **50**, 1485–1494.
21. Zimcik, P., M. Miletin, M. Kostka, J. Schwarz, Z. Musil and K. Kopecky (2004) Synthesis and comparison of photodynamic activity of alkylheteroatom substituted azaphthalocyanines. *J. Photochem. Photobiol. A, Chem* **163**, 21–28.
22. Kostka, M., P. Zimcik, M. Miletin, P. Klemra, K. Kopecky and Z. Musil (2006) Comparison of aggregation properties and photodynamic activity of phthalocyanines and azaphthalocyanines. *J. Photochem. Photobiol. A, Chem* **178**, 16–25.
23. Mørkved, E. H., N. K. Afseth and P. Zimcik (2007) Azaphthalocyanines with extended conjugation through heteroaryl and aryl substituents. Photochemical and photophysical properties. *J. Porphyr. Phthalocyanines* **11**, 130–138.
24. Donzello, M. P., E. Viola, C. Bergami, D. Dini, C. Ercolani, M. Giustini, K. M. Kadish, M. Meneghetti, F. Monacelli, A. Rosa and G. Ricciardi (2008) Tetra-2,3-pyrazinoporphyrazines with externally appended pyridine rings. 6. Chemical and redox properties and highly effective photosensitizing activity for singlet oxygen production of penta- and monopalladated complexes in dimethylformamide solution. *Inorg. Chem.* **47**, 8757–8766.
25. Kobak, R. Z. U. and A. Gül (2009) Synthesis and solution studies on azaphthalocyanines with quaternary aminoethyl substituents. *Color. Technol.* **125**, 22–28.
26. Makhseed, S., F. Ibrahim, C. G. Bezzu and N. B. McKeown (2007) The synthesis of metal-free octaazaphthalocyanine derivatives containing bulky phenoxy substituents to prevent self-association. *Tetrahedron Lett.* **48**, 7358–7361.
27. Kudrevich, S. V., M. G. Galpern, E. A. Lukyanets and J. E. vanLier (1996) Substituted tetra 2,3-pyrazinoporphyrazines. 1. Angular annelation of tetra-2,3-quinoxalino-porphyrzine. *Can. J. Chem.* **74**, 508–515.
28. Mittel, F., S. FitzGerald, A. Beeby and R. Faust (2003) Acetylenic quinoxalino-porphyrzines as photosensitisers for photodynamic therapy. *Chem. Eur. J.* **9**, 1233–1241.
29. Haas, M., S. X. Liu, A. Neels and S. Decurtins (2006) A synthetic approach to asymmetric phthalocyanines with peripheral metal-binding sites. *Eur. J. Org. Chem.*, **2006**, 5467–5478.
30. Zimcik, P., M. Miletin, Z. Musil, K. Kopecky, L. Kubza and D. Brault (2006) Cationic azaphthalocyanines bearing aliphatic tertiary amino substituents—Synthesis, singlet oxygen production and spectroscopic studies. *J. Photochem. Photobiol. A, Chem* **183**, 59–69.
31. Musil, Z., P. Zimcik, M. Miletin, K. Kopecky and J. Lenco (2007) Synthesis, separation and UV/Vis spectroscopy of pyrazinoquinoxalino-porphyrzine macrocycles. *Eur. J. Org. Chem.*, **2007**, 4535–4542.
32. Musil, Z., P. Zimcik, M. Miletin, K. Kopecky, M. Link, P. Petrik and J. Schwarz (2006) Synthesis and singlet oxygen production of azaphthalocyanines bearing functional derivatives of carboxylic acid. *J. Porphyr. Phthalocyanines* **10**, 122–131.
33. Michelsen, U., H. Kliesch, G. Schnurpfeil, A. K. Sobbi and D. Wöhrle (1996) Unsymmetrically substituted benzonaphthoporphyrazines: A new class of cationic photosensitizers for the photodynamic therapy of cancer. *Photochem. Photobiol.* **64**, 694–701.
34. Ogunsipe, A., D. Maree and T. Nyokong (2003) Solvent effects on the photochemical and fluorescence properties of zinc phthalocyanine derivatives. *J. Mol. Struct.* **650**, 131–140.
35. Seotsanyana-Mokhosi, I., T. Kresfelder, H. Abrahamse and T. Nyokong (2006) The effect of Ge, Si and Sn phthalocyanine photosensitizers on cell proliferation and viability of human oesophageal carcinoma cells. *J. Photochem. Photobiol. B-Biol.* **83**, 55–62.
36. Feofanov, A., A. Grichine, T. Karmakova, N. Kazachkina, E. Pecherskih, R. Yakubovskaya, E. Luyanets, V. Derkacheva, M. Egret-Charlier and P. Vigny (2002) Chelation with metal is not essential for antitumor photodynamic activity of sulfonated phthalocyanines. *Photochem. Photobiol.* **75**, 527–533.
37. Youngblood, W. J. (2006) Synthesis of a new trans-A(2)B(2) phthalocyanine motif as a building block for rodlike phthalocyanine polymers. *J. Org. Chem.* **71**, 3345–3356.
38. Kameyama, K., M. Morisue, A. Satake and Y. Kobuke (2005) Highly fluorescent self-coordinated phthalocyanine dimers. *Angew. Chem. Int. Ed. Engl.* **44**, 4763–4766.
39. Novakova, V., P. Zimcik, K. Kopecky, M. Miletin, J. Kuneš and K. Lang (2008) Self-assembled azaphthalocyanine dimers with higher fluorescence and singlet oxygen quantum yields than the corresponding monomers. *Eur. J. Org. Chem.* **2008**, 3260–3263.
40. Daraio, M. E., A. Völker, P. F. Aramendia and E. San Román (1996) Reaction of zinc phthalocyanine excited states with amines in cationic micelles. *Langmuir* **12**, 2932–2938.
41. Block, J. H. and J. M. Beale Jr (2004). *Wilson and Gisvold's Textbook of Organic Medicinal and Pharmaceutical Chemistry*, 11th edn. Lippincott Williams & Wilkins, Baltimore.
42. Dumin, H., T. Cernay and H. W. Zimmermann (1997) Selective photosensitization of mitochondria in HeLa cells by cationic Zn (II) phthalocyanines with lipophilic side-chains. *J. Photochem. Photobiol. B, Biol.* **37**, 219–229.